nature communications

Article

https://doi.org/10.1038/s41467-025-56838-2

Organocatalyzed diastereo- and enantioselective synthesis of N–N atropisomeric isoindolinones bearing central chirality

Received: 1 April 2024

Accepted: 3 February 2025

Published online: 15 February 2025

Check for updates

Xingguang Li[1,5] ✉, Xin-Ze Wang[1,5], Boming Shen[2,5], Qian-Yu Chen[1], Huijing Xiang[3], Peiyuan Yu[2] ✉ & Pei-Nian Liu[1,4] ✉

Methods for catalytically constructing of N–N axially chiral scaffolds have garnered significant attention since such compounds are widely present in natural products, bioactive molecules, and organic materials. Herein, we report a highly diastereoselective and enantioselective organocatalyzed [4 + 1] annulation method for synthesizing diverse valuable isoindolinones that possessing N–N axial and central chiralities. This methodology uses a chiral phosphoric acid as a bifunctional catalyst to promote a cascade sequence involving two nucleophilic additions, dehydration, and dearomatization processes. Control experiments and DFT calculations revealed a possible mechanism in which the stereoselectivity-determining step is likely to involve the irreversible formation of a hydroxy biaryl intermediate. Additionally, preliminary biological activity studies showed that some of these N–N axially chiral isoindolinones have potential in suppressing tumor-cell proliferation.

Catalytic enantioselective synthesis of atropisomers has gained substantial attention over the past few years owing to its great potential in drug discovery, catalyst/ligand design and functional material development[1–7], with significant achievements reported for the syntheses of C–C and C–N axially chiral compounds[7–26]. In sharp contrast, studies into N–N atropisomers and their syntheses remain largely underdeveloped and challenging, presumably due to the relatively low rotational barriers associated with N–N bonds. Although the N–N chiral axis is widely present in natural products, bioactive molecules, and organic materials[27–33], the Lu group first reported the construction of N–N atropisomers in 2021[34]. Since then, several strategies have been established for the construction of N–N atroposelective scaffolds (Fig. 1a)[35–48]. Organocatalyzed N–H alkylation and acylation reactions have been developed to access 1-aminopyrroles and 3-aminoquinazolinones[36–39], while, Liu realized the synthesis of N–N bispyrroles through the use of Cu-catalyzed desymmetric Friedel–Crafts alkylation chemistry[40]. In addition, asymmetric annulation chemistry involving the de novo formation of aza-arenes[41–45], and the C–H functionalization of pro-chiral N–N biaryls also provide facile access to N–N chiral bisindoles and *N*-pyrrolylindoles[46,48]. More recently, Li and Niu independently developed C–H activation/annulation for the atroposelective synthesis of *N*-aminoisoquinolinone[49,50]. Despite these advances, the development of methods for accessing novel N–N axially chiral scaffolds in a facile manner remains highly demanding yet challenging.

In recent years, the catalytic enantioselective construction of centrally chiral atropisomers has become an emerging field because it offers a significant opportunity to expand potential applications by

[1]Shanghai Key Laboratory of Functional Materials Chemistry, Key Laboratory for Advanced Materials, School of Chemistry and Molecular Engineering, East China University of Science and Technology, Shanghai 200237, China. [2]Department of Chemistry and Shenzhen Grubbs Institute, Guangdong Provincial Key Laboratory of Catalysis, Southern University of Science and Technology, Shenzhen 518055, China. [3]School of Life Sciences, Shanghai University, Shanghai 200444, China. [4]State Key Laboratory of Natural Medicines, School of Pharmacy, China Pharmaceutical University, Nanjing 210009, China. [5]These authors contributed equally: Xingguang Li, Xin-Ze Wang, Boming Shen. ✉e-mail: lixingguang@ecust.edu.cn; yupy@sustech.edu.cn; liupn@ecust.edu.cn

https://doi.org/10.1038/s41467-025-56838-2

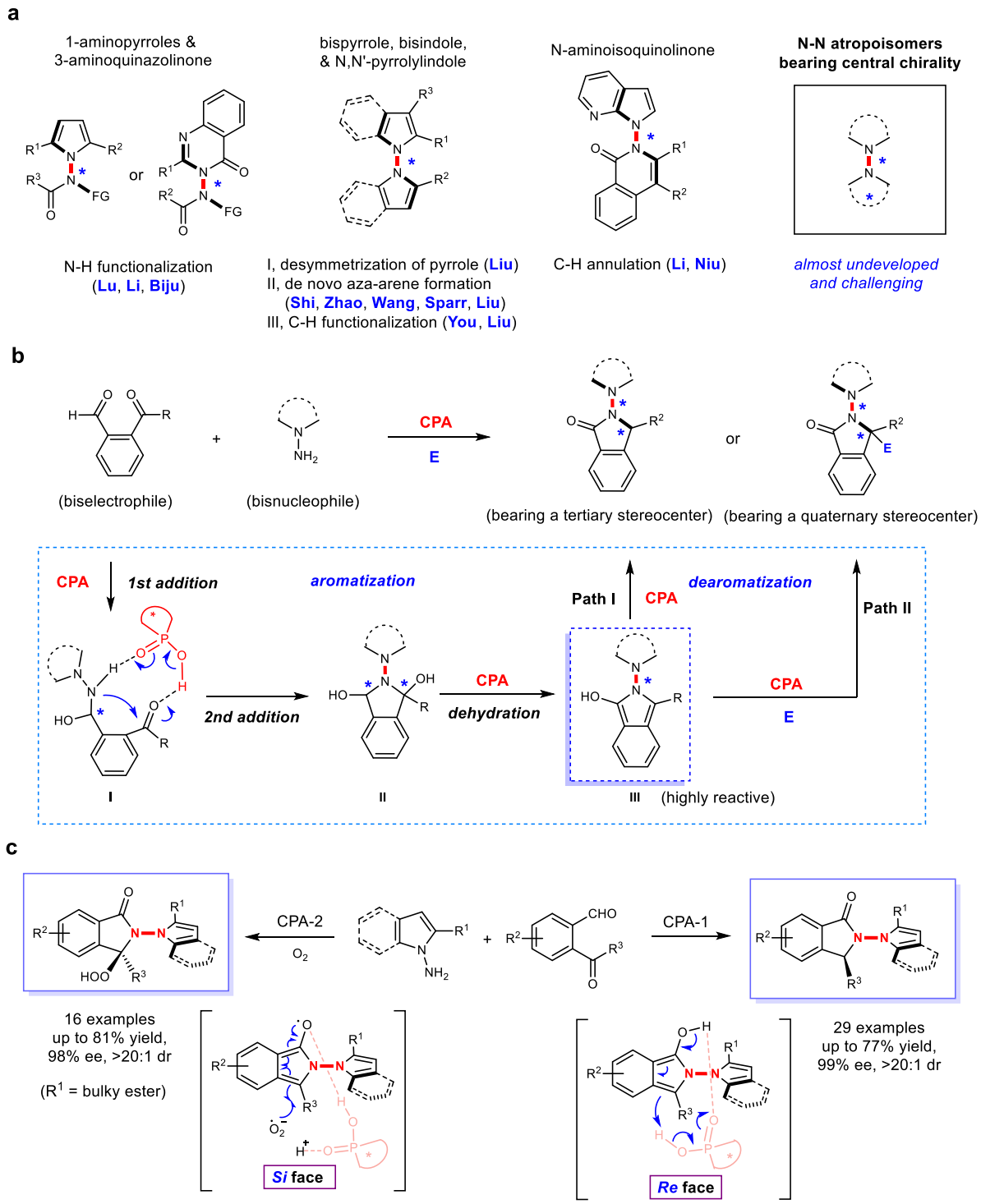

Fig. 1 | Facile synthesis of unprecedented N – N atropisomers and our design. **a** Status of catalytic construction of N – N atropisomers. **b** Concept of our design for catalytic synthesis of N – N atropisomeric isoindolinones bearing central chirality. **c** This work: synthesis of isoindolinones possessing N – N axial and central chirality. CPA chiral phosphoric acid, E electrophile.

integrating new properties into atropisomers[51–53]. In sharp contrast to the widely explored multichiral C–C and C–N atropisomers, constructing N–N atropisomers with central chirality remains largely undeveloped (Fig. 1a)[54,55]. The generation of more than one chiral element in the catalytic process presents formidable challenges for both diastereo- and enantio-control. Bencivenni recently reported chemistry for the indirect synthesis of atropoisomeric hydrazides via a one-pot sequence involving two organocatalytic cycles[54]. However,

direct approaches that provide highly stereoselective access to atropisomers bearing N–N axial and central chiralities appear to be unprecedented, despite being highly attractive.

On the other hand, isoindolinone motifs form the core structures of a variety of natural products and pharmacologically relevant molecules[56–58]. We recently became aware of a report detailing a facile access to isoindolinones by *N*-capping primary amines with 2-acylbenzaldehydes[59–61]; this transformation was assumed to involve an acid-promoted condensation-tautomerization cascade. In light of this stimulating work and recent advances in stereocontrol catalysed by chiral phosphoric acids (CPAs)[11–14,62–65], we envisaged the possibility of synthesizing N–N atropisomers by harnessing asymmetric [4 + 1] annulation chemistry involving bulky hydrazine and an *ortho*-formylbenzophenone in which contiguous axial and central chiralities are established through a CPA-catalyzed aromatization and dearomatization cascade process (Fig. 1b). In this strategy, 2-acylbenzaldehydes and hydrazines are used as 1,4-dielectrophiles and 1,1-dinucleophiles, respectively. A CPA is a suitable bifunctional catalyst that can promote sequential double nucleophilic additions and dehydration to generate reactive hydroxyisoindoline intermediate **III**, which is prone to asymmetric tautomerization (Path I). Another possible scenario involves the use of electrophilic reagents or species that can potentially react with **III** in an asymmetric dearomatization manner to furnish a N–N atropoisomer with a quaternary stereocenter (Path II). Herein, we present efficient chemistry for the synthesis of N–N atropoisomeric isoindolinones involving a highly diastereo- and enantioselective [4 + 1] annulation reaction (Fig. 1c). This transformation not only represents the first highly stereoselective and catalytic method for constructing centrally chiral N–N atropisomers, but also provides access to a new N–N atropoisomer family members that are potentially biologically active.

Results

Reaction development

To test our hypothesis, we chose 2-acyl-benzaldehyde **2a** as the 1,4-dielectrophile, *N*-aminoindole **1a** as the dinucleophile in view of its good nucleophilicity as well as the wide existence of axially chiral indole scaffolds in bioactive compounds and natural products (Table 1). To our delight, BINOL-derived CPA (*R*)-**A1** successfully catalyzed the expected asymmetric aromatization and tautomerization processes, to afford the N–N axially chiral isoindolinone **3a** in 33% yield, 25% ee, and 10:1 dr (entry 1). We next examined various BINOL- and SPINOL-derived CPA catalysts bearing aryl substituents with varying electronic properties and steric effects (entries 2–9). Among these, (*S*)-**A4** was identified as the optimal one, affording **3a** with 53% yield, 91% ee, and 13:1 dr (entry 4). Solvent screening (see the Supplementary Information for details) showed that *o*-xylene and PhCl performed competitively, whereas DCE led to a sharp decrease in ee, albeit with a higher yield (entries 10–12). Toluene was determined to be the best solvent. Moreover, an enhanced yield and a slightly higher ee were obtained by decreasing the temperature to −20 °C (entry 13). Finally, reducing the catalyst loading to 5 mol% improved the yield to 73%, along with 93% ee and >20:1 dr (entry 14). It is worth mentioning that by-product **3a'** was observed in yields of less than 10% in these optimization studies (see the Supplementary Information for details)[66].

Substrates scope exploration

Having identified the optimal conditions (entry 14, Table 1), we next examined the scope of the asymmetric [4 + 1] annulation reaction (Fig. 2). A wide range of *N*-aminoindoles **1** bearing substituents with different electronic properties at the C5, C4, and C3 positions exhibited good reactivities in this reaction, with products **3a**–**3k** formed in yields of 54–77% with excellent enantioselectivities and diastereoselectivities (89–98% ee, >20:1 dr). Other ester and even amide groups at the C2 position of the indole ring were also tolerated, to afford **3 l** and **3 m** in moderate-to-good yields and high stereoselectivities. To further broaden the substrate scope, we also examined *N*-aminopyrroles. To ensure that a sufficiently rotationally restricted N–N axis was generated, we initially examined the use of 2,4-disubstituted *N*-aminopyrrole **1n**. Gratifyingly, the desired product **3n** was efficiently formed (64% yield, >99% ee, >20:1 dr) using (*R*)-**C2** as the catalyst. Moreover, multi-substituted *N*-aminopyrroles also performed well to afford **3o** and **3p**. In addition, various ester units were well tolerated in this system, with **3q**–**3t** produced in good yields and excellent stereoselectivities (56–72% yield, 94–96% ee, >20:1 dr). The absolute configurations of **3i** and **3n** were assigned to be ($R_{N\text{-}N}$, S_C) and ($R_{N\text{-}N}$, R_C), respectively, by X-ray crystallography.

We next studied the feasibility of asymmetric [4 + 1] annulation chemistry involving different 2-acylbenzaldehydes. A variety of 2-acetylbenzaldehydes bearing substituents with different electronic properties at the C4–C6 positions reacted smoothly with **1a** to highly efficiently and stereoselectively afford N–N axially chiral isoindolinones **3u**–**3aa** (57–74% yield, 88–99% ee, >20:1 dr). Changing of the methyl group to *n*-propyl did not significantly affect the efficiency or stereoselectivity of the reaction.

In addition, we also attempted to construct a contiguous N–N axis and quaternary stereocenter by harnessing an appropriate electrophile to trap the in-situ generated hydroxyisoindoline intermediate **III** in presence of a CPA; however, our efforts were unsuccessful. The enol species significantly favored tautomerization over nucleophilic addition in the acidic system. Interestingly, *N*-aminoindole **1** bearing a bulky $CO_2{}^{i}Pr$ or $CO_2{}^{t}Bu$ ester moiety at the C2 position, underwent an unexpected condensation and oxidative asymmetric dearomatization (Fig. 3). This transformation predominantly delivered N–N axially chiral isoindolinonyl hydroperoxide **4a** or **4b** bearing a quaternary stereocenter with excellent stereoselectivities (92–97% ee, >20:1 dr). The structure and absolute configuration of **4b** were confirmed by X-ray crystallography. We subsequently expanded the scope of this chiral isoindolinonyl hydroperoxide-forming chemistry; 2-acylbenzaldehydes bearing either electron-donating or electron-withdrawing groups performed well in this transformation, to highly efficiently yield **4c**–**4 f** with excellent stereoselectivities. A *n*-propyl or aryl substituent was well tolerated, rendering products **4g**–**4k** with high efficiency (56–64% yields, 85–96% ee and >20:1 dr), irrespective of the electronic nature or position of the substituent on the phenyl ring. The protocol also tolerated 5-methyl- and 5-bromo-substituted *N*-aminoindoles, furnishing **4l**–**4o** in moderate-to-good yields with excellent stereocontrol (94–98% ee, >20:1). Also, **1 y**, which is derived from (−)-borneol, was a suitable substrate for preparing **4p**, albeit in notably lower yield.

Moreover, the chiral products **3p**, **3 u**, **4 f** and **4j** were stirred in toluene at 110 °C for 12 h. Such four compounds could be recovered in high yields, with high enantioselectivities and diastereoselectivities retained, which indicated that the N–N axially chiral isoindolinones have high chemical stability and configurational stability (see the Supplementary Information for details).

Synthetic applications and mechanistic studies

To further highlight the synthetic practicality and utility of this catalytic method, we performed scaled-up experiments and further transformed the chiral products (Fig. 4). **1e** was reacted with **2a**, while **1o** was reacted with **2a**, each on a 1 mmol scale, with products **3e** and **3n** obtained without obvious erosions in yield or stereoselectivity (Fig. 4a, b). In addition, selective C3-bromination of the pyrrole ring of **3n** proceeded well to form **3p**, which underwent further Suzuki-coupling with minimal erosion of enantiopurity (Fig. 4c). The ester substituent in **3n** was readily converted into a carboxyl group, with the high ee of the starting material maintained.

https://doi.org/10.1038/s41467-025-56838-2

Table 1 | Optimization of the reaction conditions[a]

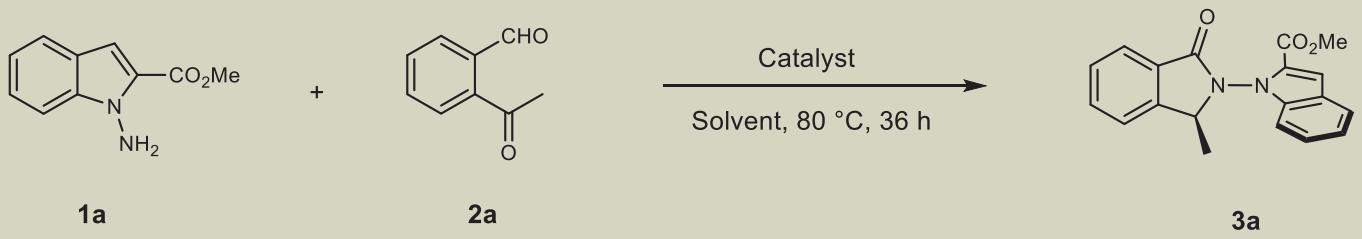

1a **2a** **3a**

Entry	Catalyst	Solvent	Yield (%)[b]	ee (%)[c]	dr[d]
1	(*R*)-**A1**	Toluene	33	−25	10:1
2	(*R*)-**A2**	Toluene	23	−7	17:1
3	(*R*)-**A3**	Toluene	54	−26	12:1
4	(*S*)-**A4**	Toluene	53	91	13:1
5	(*R*)-**B1**	Toluene	56	−22	12:1
6	(*R*)-**B2**	Toluene	60	−9	10:1
7	(*R*)-**B3**	Toluene	42	−40	15:1
8	(*R*)-**C1**	Toluene	trace	ND	ND
9	(*R*)-**C2**	Toluene	trace	ND	ND
10	(*S*)-**A4**	DCE	63	28	8:1
11	(*S*)-**A4**	*o*-Xylene	50	89	10:1
12	(*S*)-**A4**	PhCl	51	89	10:1
13[e]	(*S*)-**A4**	Toluene	65	92	>20:1
14[e, f]	(*S*)-**A4**	Toluene	73	93	>20:1
15[e, g]	(*S*)-**A4**	Toluene	61	91	>20:1

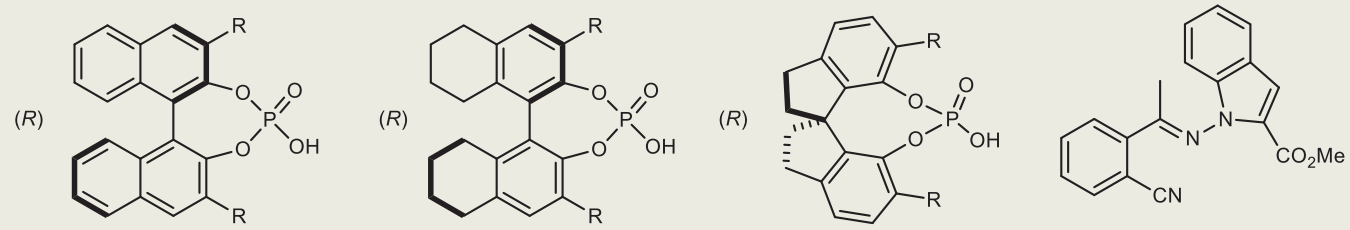

A1: R = 1-naphthyl
A2: R = 9-anthracenyl
A3: R = $SiPh_3$
A4: R = 2,4,6-(^{i}Pr)$_3$C$_6$H$_2$

B1: R = 1-naphthyl
B2: R = 9-anthraceny
B3: R = 2,4,6-(^{i}Pr)$_3$C$_6$H$_2$

C1: R = 9-anthracenyl
C2: R = 2,4,6-(^{i}Pr)$_3$C$_6$H$_2$

3a'

[a]Reaction conditions: **1a** (0.1 mmol), **2a** (0.05 mmol), catalyst (10 mol%), toluene (0.5 mL).
[b]Isolated yields are provided.
[c]The ee values were determined by chiral HPLC.
[d]Diastereomeric ratios (dr) were determined from ^{1}H NMR of the isolated product.
[e]Reaction performed at −20 °C.
[f]5 mol% of (*S*)-**A4** was used.
[g]2.5 mol% of (*S*)-**A4** was used. DCE, 1,2-dichloroethane; PhCl, chlorobenzene.

A series of control experiments were carried out to gain some insights into the reaction mechanism (Fig. 5). First, phthalaldehyde was reacted with **1e** to form the desired product **7**, whereas the 1,2-diacetylbenzene reacted with **1e** to afford a complex mixture with no cyclized compound detected (Fig. 5, eq 1 and 2), which indicates that dehydration is essential for the [4 + 1] annulation reaction. Moreover, treating side product **3a'** with H_2O (1 equiv.) under typical conditions did not afford **3a** (Fig. 5, eq 3), which suggests that **3a'** is not a reaction intermediate. Interestingly, replacing the CPA catalyst with achiral diphenylphosphoric acid provided racemic products **3i** and **3n** with excellent diastereoselectivities (Fig. 5, eq 4 and 5). In addition, we treated **4 d'** under the standard conditions to shed light on the formation of hydroperoxide; **4 d** was not formed under these conditions, thereby excluding the involvement of a direct oxidation pathway (Fig. 5, eq 6). Some deuterium experiments were conducted (see the Supplementary Information for details). We introduced **RPA1-D** to the reaction of **1a** and **2a**, providing product **3a** in 53% yield with 24% deuterium incorporation. The result indicates that CPA works as an acid and proton source in the reaction for **3a**.

https://doi.org/10.1038/s41467-025-56838-2

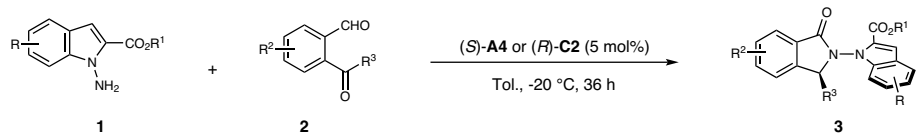

1 2 3

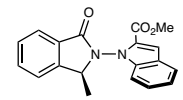

3a, 68%, 93% ee, >20:1 dr

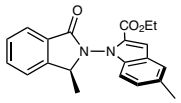

3b, 61%, 93% ee, >20:1 dr

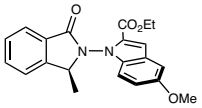

3c, 77%, 94% ee, >20:1 dr

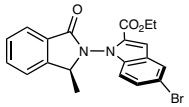

3d, 60%, 96% ee, >20:1 dr

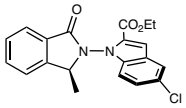

3e, 69%, 97% ee, >20:1 dr

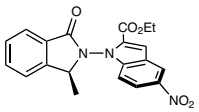

3f, 62%, 96% ee, >20:1 dr

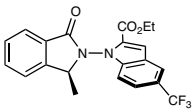

3g, 58%, 94% ee, >20:1 dr

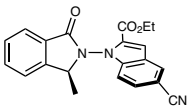

3h, 62%, 98% ee, >20:1 dr

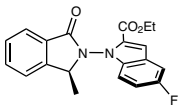

3i, 54%, 97% ee, >20:1 dr

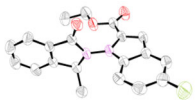

X-ray structure of **3i**

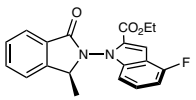

3j, 55%, 89% ee, >20:1 dr

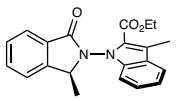

3k, 66%, 94% ee, >20:1 dr

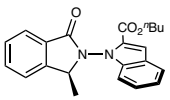

3l, 69%, 85% ee, >20:1 dr

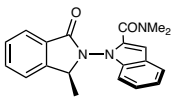

3m, 52%, 87% ee, 8:1 dr

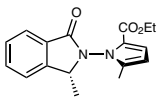

3n, 64%, >99% ee, >20:1 dr[a]

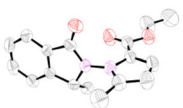

X-ray structure of **3n**

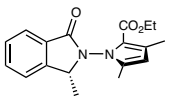

3o, 57%, 96% ee, >20:1 dr[a]

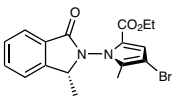

3p, 69%, 98% ee, >20:1 dr[a]

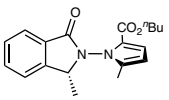

3q, 70%, 95% ee, >20:1 dr[a]

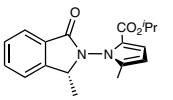

3r, 72%, 96% ee, >20:1 dr[a]

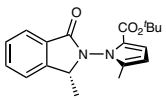

3s, 56%, 95% ee, >20:1 dr[a]

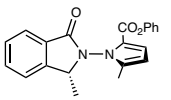

3t, 62%, 94% ee, >20:1 dr[a]

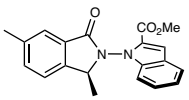

3u, 74%, 93% ee, >20:1 dr

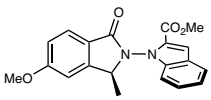

3v, 57%, 88% ee, >20:1 dr

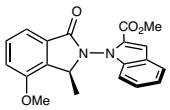

3w, 69%, 96% ee, >20:1 dr

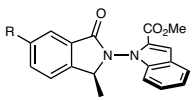

3x, R = F, 60%, >99% ee, >20:1 dr
3y, R = CF_3, 63%, 92% ee, >20:1 dr

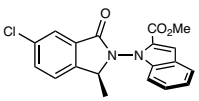

3z, 73%, 98% ee, >20:1 dr

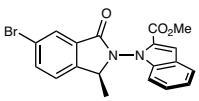

3aa, 66%, 94% ee, >20:1 dr

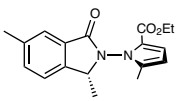

3ab, 61%, 95% ee, >20:1 dr[a]

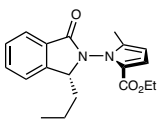

3ac, 68%, 84% ee, >20:1 dr[a]

Fig. 2 | Scope of the asymmetric [4 + 1] annulation for N–N axially chiral isoindolinones. Reaction conditions: **1** (0.4 mmol), **2** (0.2 mmol), (*S*)-**A4** (5 mol%), toluene (2 mL), −20 °C, 36 h. Isolated yields. [a](*R*)-**C2** (5 mol%) was used as catalyst, 25 °C, 24 h. Tol., toluene.

Density functional theory studies

We used density functional theory (DFT) calculations to model the formation of isoindolinone **3a** by the reaction of hydrazine **1a** with 2-acylbenzaldehyde **2a** to better understand the mechanism and key steps responsible for the observed stereoselectivity. As shown in Fig. 6a, the first addition of the amino group of **1a** to the aldehyde reversibly generates racemic intermediate **I**, which is 1.4 kcal/mol higher in energy than the reactants. The second addition to the ketone moiety forms intermediate **II**, which contains two chiral centers and one chiral axis. Consequently, eight stereoisomers are possible. The relative energies of the four diastereomers range from −3.5 to −0.6 kcal/mol (Fig. 6b). The subsequent dehydration and tautomerization, which generates intermediate **III** and product **3a**, respectively, are highly exergonic and irreversible. The calculated rotational barriers for intermediates **II**, **III**, and **3a** are shown in Fig. 6c. The irreversible formation of intermediate **III** is highly likely to be the stereodetermining step owing to the calculated high barriers, leading to the formation of only one major enantiomer of **III**. The exact process by which the chiral phosphoric acid catalyst facilitates this step and controls the stereoselectivity is currently being explored in our laboratories.

Additionally, we propose a plausible mechanism for the formation of products **3** and **4** based on our experimental observations and the DFT calculations discussed above, as well as literature precedent

https://doi.org/10.1038/s41467-025-56838-2

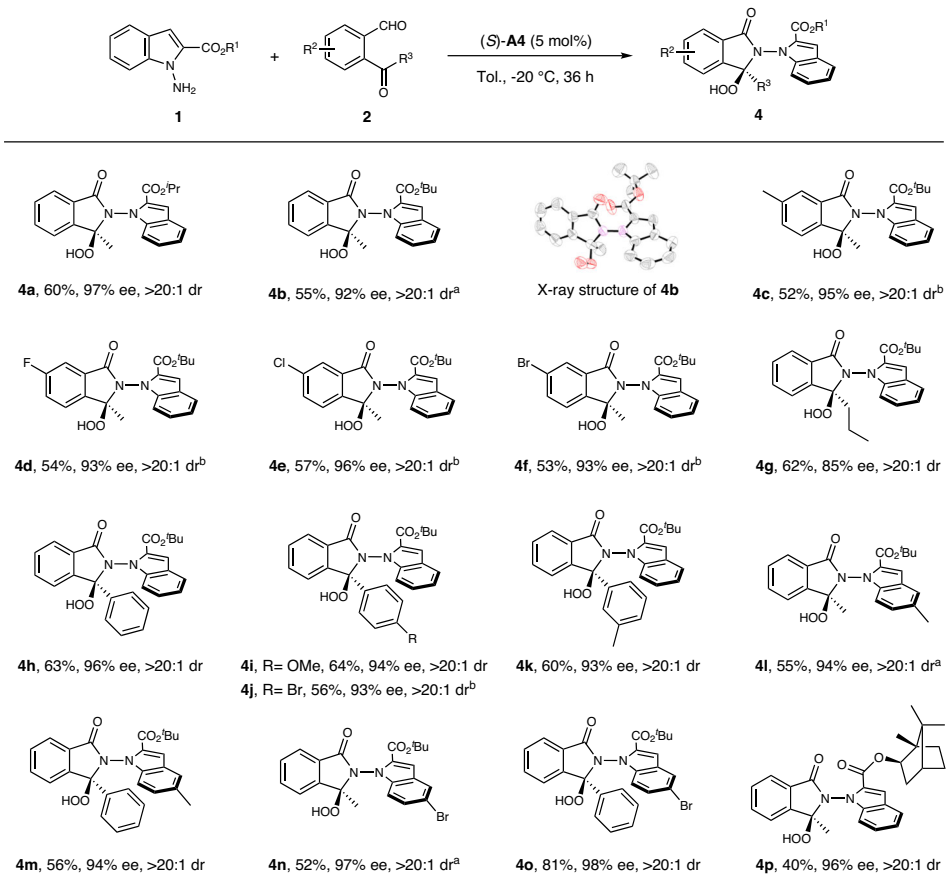

Fig. 3 | Scope of N–N axially chiral isoindolinones bearing a quaternary stereocenter. Reaction conditions: **1** (0.4 mmol), **2** (0.2 mmol), (*S*)-**A4** (5 mol%), toluene (2 mL), −20 °C, 36 h. Isolated yields. [a]0 °C, 72 h. [b]*p*-Xylene, 25 °C, 24 h.

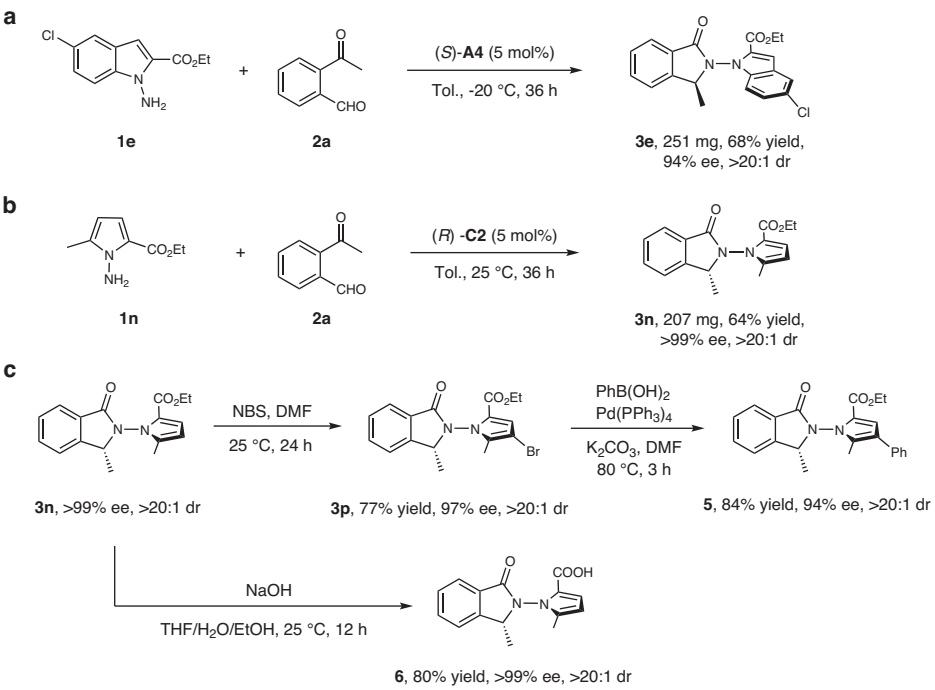

Fig. 4 | Scale-up experiments and synthetic application. a, b Mmol-scale synthesis. **c** Transformations of enantioenriched products. NBS *N*-Bromosuccinimide, DMF *N*,*N*-Dimethylformamide, THF tetrahydrofuran.

https://doi.org/10.1038/s41467-025-56838-2

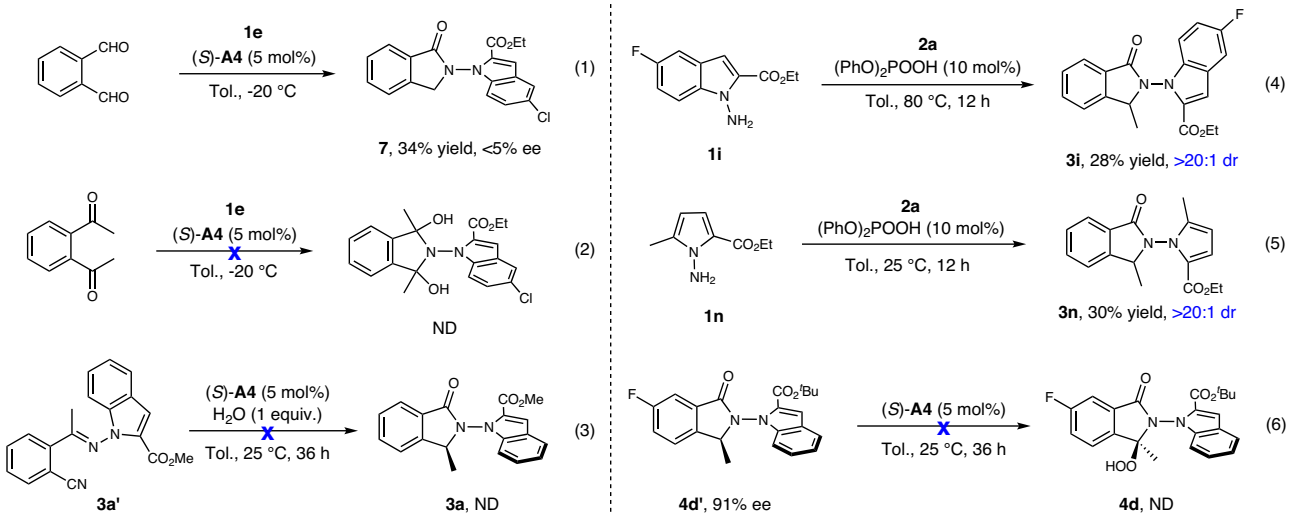

Fig. 5 | Control experiments. Control experiments for the [4+1] annulation or the oxidation process.

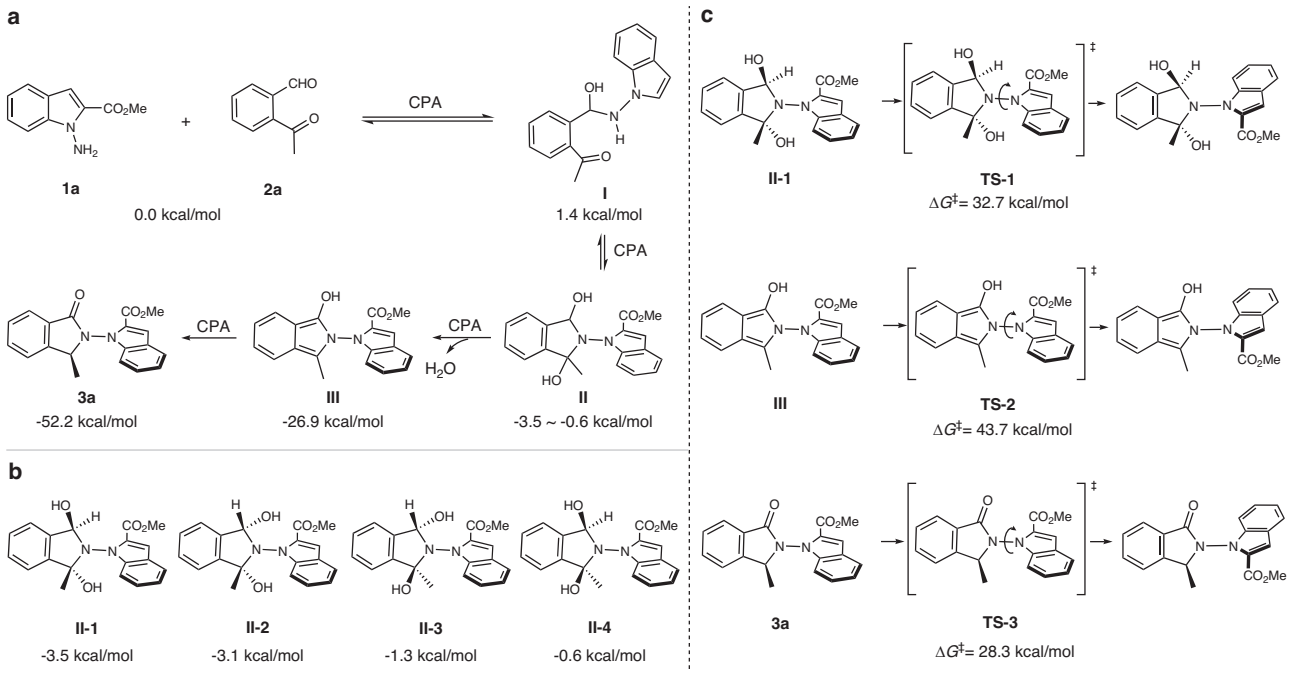

Fig. 6 | DFT calculations for the reaction free energies of model reaction between 1a and 2a to form product 3a. a The energy profile of the [4 + 1] annulation of **1a** and **2a**. **b** The relative energies of the four different diastereomers **II-1** – **II-4**. **c** The computed rotational barriers of intermediates **II, III**, and product **3a**.

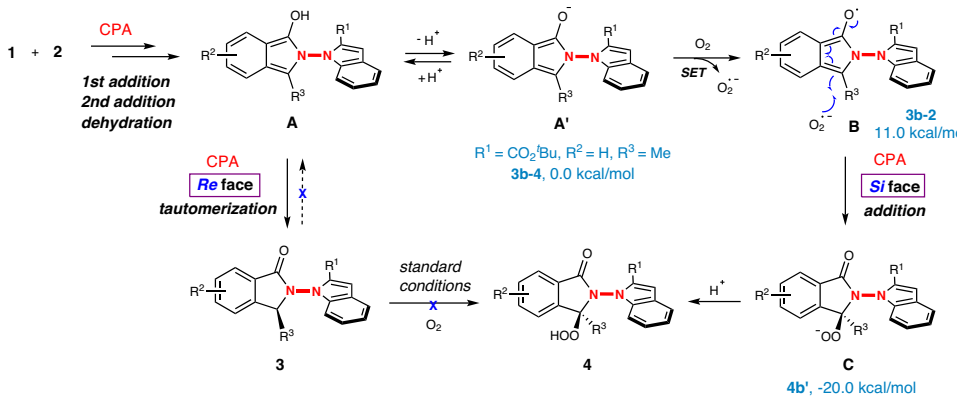

Fig. 7 | Proposed mechanism for the generation of products 3 and 4. Plausible mechanism.

https://doi.org/10.1038/s41467-025-56838-2

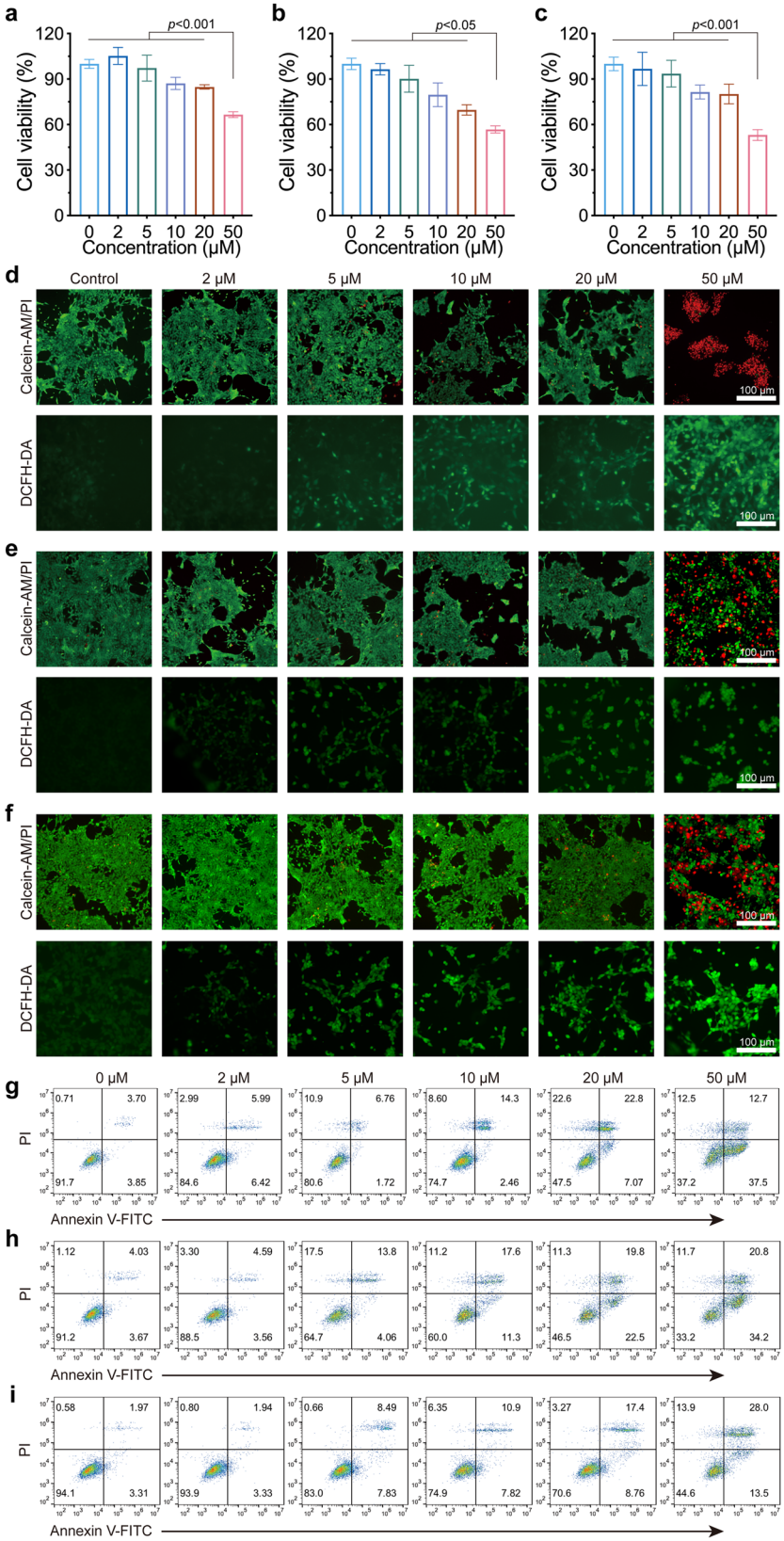

Fig. 8 | Anticancer performance assessment. a–c Cell viability of compounds **3a, 3n**, and **4a** (n = 5 biologically independent samples). **d–f** Confocal images of 4T1 cells stained with DCFH-DA and calcein-AM/PI after treatment with various doses of compounds **3a, 3n**, and **4a**. **g–i** Flow cytometry analysis of apoptotic cells after treatment with different concentrations of compounds **3a, 3n**, and **4a**.

(Fig. 7)[40–54,67,68]. The process begins with acid-promoted addition and dehydration to form intermediate **A**, which tautomerizes by protonation at the *Re* face of the hydroxypyrrole-ring plane to give product **3**. Alternatively, it is proposed that the oxidative dearomatizaion is initiated by the removal of a proton and the triplet O_2 is more likely to oxidize the generated anion **A'** to a radical species **B** through a single-electron transfer (SET) process[67,68]. Subsequently, the residual superoxide radical anion attacks the C4 position of the pyrrole ring of intermediate **B** from the *Si* face to form **C**, which is finally protonated to afford product **4**. Preliminary results from DFT-calculated energetics suggest that this mechanism is feasible. The theoretical result indicated that the deprotonated anion **3b-4** is much easier to be oxidized by triplet oxygen through a SET process to generate radical **3b-2**, which is endergonic by 11.0 kcal/mol. The subsequent addition of the superoxide radical anion to radical **3b-2** is highly exergonic (-31.0 kcal/mol), which provides the driving force for the whole process. Moreover, we have performed additional DFT calculations to investigate the thermodynamic preferences for the two types of products (see the Supplementary Information for details). The preliminary results indicate that the formation of **3a** (*Re* face) is thermodynamically preferred. In contrast, the observed product (**4b**) for the peroxidation (*Si* face) is less stable than the minor diastereomer **4b-1**, which suggests that the CPA catalyst is likely involved in the peroxidation step.

Anticancer performance evaluation

Finally, we were intrigued by the potential biological activities of the synthesized enantioenriched N − N atropisomers. Isoindolinones exhibited various biological activities, including anticancer, antibacterial, antiviral activities, and have been extensively studied as key core scaffolds for diverse drug candidates[69–73]. Therefore, it is of crucial significance to assess the antitumor performance of our synthesized N − N axially chiral isoindolinones, as shown in Figs. 2, 3. Cell counting kit-8 (CCK-8) assay was used to preliminarily screen the viability of 4T1 cell after treatment with a series of products **3** and **4**. The results of CCK-8 illustrated that compounds **3a**, **3n**, and **4a** partially inhibited tumor-cell growth, with the cell viabilities of 66.5%, 56.8%, and 53.1% at the concentration of 50 μM, respectively (Fig. 8a–c). These preliminary results shown that our synthesized N − N axially chiral isoindolinones have potential in inhibiting tumor-cell growth.

Generally, overproduction of reactive oxygen species (ROS) is a key marker in the early stage of apoptotic cells. 2′,7′-dichlorodihydrofluorescein diacetate (DCFH-DA) was utilized as the ROS fluorescent probe to assess the intracellular ROS levels after diverse treatments. As displayed in Fig. 8d–f, the confocal images illustrated that the green fluorescence signals of ROS increased with elevating doses of compounds **3a**, **3n**, and **4a**, indicating the effective apoptosis induction. Furthermore, 4T1 cells were treated with increasing concentrations of these compounds, and then labeled with calcein acetoxymethyl ester (calcein-AM) and propidium iodide (PI) to visualize live and dead cells. After treatment with 50 μM of **3a**, **3n**, and **4a**, a distinct red fluorescence signal of PI was observed in 4T1 cells, suggesting their high inhibitory activity against cancer cells. Moreover, flow cytometry analysis was conducted using annexin V-fluorescein isothiocyanate/PI (annexin V-FITC/PI) staining assay to confirm the apoptosis induction by these three compounds (Fig. 8g–i). The results revealed that compounds **3a**, **3n**, and **4a** induced apoptosis of 4T1 cells in a dose-dependent manner, with apoptosis rates of 50.2%, 55% and 41.5% at 50 μM, respectively, which verified that the anticancer activity of compounds **3a**, **3n**, and **4a** may be related to the induction of apoptosis.

Discussion

In summary, we established an unprecedented, highly diastereoselective, and atroposelective protocol for the synthesis of N–N axially chiral isoindolinones that proceeds via a Brønsted acid-catalyzed asymmetric [4 + 1] annulation, which represents the first example of the direct construction of N–N atropisomers with central chirality and excellent stereocontrol. This methodology is promoted by a chiral phosphoric acid that bifunctionally catalyzes a sequence of two nucleophilic additions, dehydration, and dearomatization. Control experiments and DFT calculations revealed that the mechanism possibly involves the irreversible formation of the hydroxy-biaryl intermediate as likely the key step responsible for the observed stereoselectivity. In addition, preliminary biological activity studies revealed that some of these N–N axially chiral isoindolinones exhibited potential tumor-cell inhibitory activity.

Methods

General procedure for the synthesis of enantioenriched 3 and 4

General Procedure. At −20 °C or 25 °C, to an oven-dried 10-mL vial charged with a solution of the 1*H*-indol-1-amine or 2-methyl-1*H*-pyrrol-1-amine **1** (0.4 mmol) and the substituted 2-acetylbenzaldehyde **2a** (0.2 mmol) in toluene (1.5 mL) was added a solution of the catalyst (*S*)-**A4** (7.5 mg, 0.01 mmol, 5 mol%) or (*R*)-**C2** (6.7 mg, 0.01 mmol, 5 mol%) in toluene (0.5 mL). The reaction mixture was stirred at the same temperature for 24 h or 36 h. The mixture was concentrated under reduced pressure and then purified by silica gel (deactivated by triethylamine) flash chromatography to afford the desired product **3** or **4**.

Reporting summary

Further information on research design is available in the Nature Portfolio Reporting Summary linked to this article.

Data availability

All data generated and analyzed during this study are included in this Article and its Supplementary Information. The X-ray crystallographic coordinate for structures **3i**, **3n**, and **4b** have been deposited at the Cambridge Crystallographic Data Centre under deposition numbers CCDC 2323929 (for **3i**), 2323930 (for **3n**), and 2323931 (for **4b**), respectively and can be obtained free of charge from the CCDC via http://www.ccdc.cam.ac.uk/data_request/cif. All data are available from the corresponding author upon request. Source data are present with this paper. Source data are provided with this paper.

References

1. Bringmann, G., Gulder, T., Gulder, T. A. M. & Breuning, M. Atroposelective total synthesis of axially chiral biaryl natural products. *Chem. Rev.* **111**, 563–639 (2011).
2. Toenjes, S. T. & Gustafson, J. L. Atropisomerism in medicinal chemistry: challenges and opportunities. *Future Med. Chem.* **10**, 409–422 (2018).
3. Perreault, S., Chandrasekhar, J. & Patel, L. Atropisomerism in drug discovery: A medicinal chemistry perspective inspired by atropisomeric class I PI3K inhibitors. *Acc. Chem. Res.* **55**, 2581–2593 (2022).
4. Zhou, Q.-L. *Privileged Chiral Ligands and Catalysts* (Wiley, 2011).
5. Da, B.-C. & Tan, B. *Application for axially chiral ligands. In axially chiral compounds: Asymmetric synthesis and applications part II* (Wiley, 2021).
6. Erbas-Cakmak, S., Leigh, D. A., McTernan, C. T. & Nussbaumer, A. L. Artificial molecular machines. *Chem. Rev.* **115**, 10081–10206 (2015).
7. Kumarasamy, E., Raghunathan, R., Sibi, M. P. & Sivaguru, J. Nonbiaryl and heterobiaryl atropisomers: molecular templates with promise for atropselective chemical transformations. *Chem. Rev.* **115**, 11239–11300 (2015).
8. Wencel-Delord, J., Panossian, A., Leroux, F. R. & Colobert, F. Recent advances and new concepts for the synthesis of axially stereoenriched biaryls. *Chem. Soc. Rev.* **44**, 3418–3430 (2015).
9. Link, A. & Sparr, C. Stereoselective arene formation. *Chem. Soc. Rev.* **47**, 3804–3815 (2018).

10. Metrano, A. J. & Miller, S. J. Peptide-Based catalysts reach the outer sphere through remote desymmetrization and atroposelectivity. *Acc. Chem. Res.* **52**, 199–215 (2019).
11. Zhang, Y.-C., Jiang, F. & Shi, F. Organocatalytic asymmetric synthesis of indole-based chiral heterocycles: strategies, reactions, and outreach. *Acc. Chem. Res.* **53**, 425–446 (2020).
12. Shao, Y.-D. & Cheng, D.-J. Chiral phosphoric acid: A powerful organocatalyst for the asymmetric synthesis of heterocycles with chiral atropisomerism. *ChemCatChem* **13**, 1271–1289 (2021).
13. Cheng, J. K., Xiang, S.-H., Li, S., Ye, L. & Tan, B. Recent advances in catalytic asymmetric construction of atropisomers. *Chem. Rev.* **121**, 4805–4902 (2021).
14. Cheng, J. K., Xiang, S.-H. & Tan, B. Organocatalytic enantioselective synthesis of axially chiral molecules: Development of strategies and skeletons. *Acc. Chem. Res.* **55**, 2920–2937 (2022).
15. Sheng, F.-T., Yang, S., Wu, S.-F., Zhang, Y.-C. & Shi, F. Catalytic asymmetric synthesis of axially chiral 3,3′-bisindoles by direct coupling of indole rings. *Chin. J. Chem.* **40**, 2151–2160 (2022).
16. Hang, Q.-Q. et al. Design and catalytic atroposelective synthesis of axially chiral isochromenone-indoles. *Sci. China Chem.* **65**, 1929–1937 (2022).
17. Liu, Y.-W., Chen, Y.-H., Cheng, J. K., Xiang, S.-H. & Tan, B. Enantioselective synthesis of 3-arylindole atropisomers via organocatalytic indolization of iminoquinones. *Chem. Synth.* **3**, 1–8 (2023).
18. Zhang, X., Zhao, K. & Gu, Z. Transition metal-catalyzed biaryl atropisomer synthesis via a torsional strain promoted ring-opening reaction. *Acc. Chem. Res.* **55**, 1620–1633 (2022).
19. Portolani, C., Centonze, G., Righi, P. & Bencivenni, G. Role of cinchona alkaloids in the enantio- and diastereoselective synthesis of axially chiral compounds. *Acc. Chem. Res.* **55**, 3551–3571 (2022).
20. Li, T.-Z., Liu, S.-J., Tan, W. & Shi, F. Catalytic asymmetric construction of axially chiral indole-based frameworks: an emerging area. *Chem. Eur. J.* **26**, 15779–15792 (2020).
21. Kitagawa, O. Chiral Pd-catalyzed enantioselective syntheses of various N–C axially chiral compounds and their synthetic applications. *Acc. Chem. Res.* **54**, 719–730 (2021).
22. Colobert, F. & Shi, B.-F. C–N atropopure compounds: new directions. *Chem. Catal.* **1**, 483–485 (2021).
23. Zhang, H.-H. & Shi, F. Organocatalytic atroposelective synthesis of indole derivatives bearing axial chirality: strategies and applications. *Acc. Chem. Res.* **55**, 2562–2580 (2022).
24. Wu, Y.-J., Liao, G. & Shi, B.-F. Stereoselective construction of atropisomers featuring a C–N chiral axis. *Green Synth. Catal.* **3**, 117–136 (2022).
25. Rodríguez-Salamanca, P., Fernández, R., Hornillos, V. & Lassaletta, J. M. Asymmetric synthesis of axially chiral C–N atropisomers. *Chem. Eur. J.* **28**, e202104442 (2022).
26. Zhang, X. K., Liu, Y.-Z., Shao, H. W. & Ma, X. F. Advances in atroposelectively de novo synthesis of axially chiral heterobiaryl scaffolds. *Molecules* **27**, 8517 (2022).
27. Zhang, Q. et al. N–N-Coupled indolo-sesquiterpene atropo-diastereomers from a marine-derived actinomycete. *Eur. J. Org. Chem.* **2012**, 5256–5262 (2012).
28. Xu, Z., Baunach, M., Ding, L. & Hertweck, C. Bacterial synthesis of diverse indole terpene alkaloids by an unparalleled cyclization sequence. *Angew. Chem. Int. Ed.* **51**, 10293–10297 (2012).
29. Blair, L. M. & Sperry, J. Natural products containing a nitrogen–nitrogen bond. *J. Nat. Prod.* **76**, 794–812 (2013).
30. Klein, J. T. et al. Synthesis and structure-activity relationships of *N*-propyl-*N*-(4-pyridinyl)-1*H*-indol-1-amine (besipirdine) and related analogs as potential therapeutic agents for alzheimer's disease. *J. Med. Chem.* **39**, 570–581 (1996).
31. Shoeb, M. et al. Isolation, structure elucidation and bioactivity of schischkiniin, a unique indole alkaloid from the seeds of centaurea schischkinii. *Tetrahedron* **61**, 9001–9006 (2005).
32. Suzuki, K., Nomura, I., Ninomiya, M., Tanaka, K. & Koketsu, M. Synthesis and antimicrobial activity of β-carboline derivatives with N^2-alkyl modifications. *Bioorg. Med. Chem. Lett.* **28**, 2976–2978 (2018).
33. Liu, X.-Y., Zhang, Y.-L., Fei, X., Liao, L.-S. & Fan, J. 9,9′-Bicarbazole: New molecular skeleton for organic light emitting diodes. *Chem. Eur. J.* **25**, 4501–4508 (2019).
34. Mei, G.-J. et al. Rational design and atroposelective synthesis of N–N axially chiral compounds. *Chem.* **7**, 2743–2757 (2021).
35. Centonze, G., Portolani, C., Righi, P. & Bencivenni, G. Enantioselective strategies for the synthesis of N–N atropisomers. *Angew. Chem. Int. Ed.* **62**, e202303966 (2023).
36. Lin, W. et al. Asymmetric synthesis of N–N axially chiral compounds via organocatalytic atroposelective *N*-acylation. *Chem. Sci.* **13**, 141–148 (2022).
37. Balanna, K. et al. N-heterocyclic carbene-catalyzed atroposelective synthesis of N–N axially chiral 3-amino quinazolinones. *ACS Catal.* **13**, 8752–8759 (2023).
38. Song, C. Y. et al. Catalytic *N*-acylation for access to N – N atropisomeric *N*-aminoindoles: choice of acylation reagents and mechanistic insights. *ACS Catal.* **14**, 6926–6935 (2024).
39. Ranganathappa, S. S. et al. Atroposelective synthesis of N – N axially chiral indoles and pyrroles via NHC-catalyzed diastereoselective (3 + 3) annulation strategy. *ACS Catal.* **14**, 6965–6972 (2024).
40. Wang, X.-M. et al. Enantioselective synthesis of nitrogen–nitrogen biaryl atropisomers via copper-catalyzed Friedel-Crafts alkylation reaction. *J. Am. Chem. Soc.* **143**, 15005–15010 (2021).
41. Chen, K.-W. et al. Organocatalytic atroposelective synthesis of N – N axially chiral indoles and pyrroles by de novo ring formation. *Angew. Chem. Int. Ed.* **61**, e202116829 (2022).
42. Chen, Z.-H. et al. Organocatalytic enantioselective synthesis of axially chiral *N*,*N*′-bisindoles. *Angew. Chem. Int. Ed.* **62**, e202300419 (2023).
43. Gao, Y. et al. Atroposelective synthesis of 1,1′-bipyrroles bearing a chiral N – N axis: chiral phosphoric acid catalysis with lewis acid induced enantiodivergence. *Angew. Chem. Int. Ed.* **61**, e202200371 (2022).
44. Yang, G. M., He, Y., Wang, T. Y., Li, Z. P. & Wang, J. Atroposelective synthesis of planar-chiral indoles via carbene catalyzed macrocyclization. *Angew. Chem. Int. Ed.* **63**, e202316739 (2024).
45. Hutskalova, V. & Sparr, C. Control over stereogenic N–N axes by Pd-Catalyzed 5-endo-hydroaminocyclizations. *Synthesis* **55**, 1770–1782 (2023).
46. Zhang, P. et al. Enantioselective synthesis of N – N bisindole atropisomers. *Angew. Chem. Int. Ed.* **61**, e202212101 (2022).
47. Yin, S.-Y., Zhou, Q., Liu, C.-X., Gu, Q. & You, S.-L. Enantioselective synthesis of N–N biaryl atropisomers through iridium(I)-catalyzed C–H alkylation with acrylates. *Angew. Chem. Int. Ed.* **62**, e202305067 (2023).
48. Yao, W. et al. Enantioselective synthesis of N – N atropisomers by palladium-catalyzed C – H functionalization of pyrroles. *Angew. Chem. Int. Ed.* **62**, e202218871 (2023).
49. Wang, Y.-S. et al. Rhodium-catalyzed enantioselective and diastereodivergent access to diaxially chiral heterocycles. *Nat. Commun.* **14**, 4661 (2023).
50. Li, T. et al. Cobalt-catalyzed atroposelective C – H activation/annulation to access N – N axially chiral frameworks. *Nat. Commun.* **14**, 5271 (2023).
51. Bai, X.-F., Cui, Y.-M., Cao, J. & Xu, L.-W. Atropisomers with axial and point chirality: Synthesis and applications. *Acc. Chem. Res.* **55**, 2545–2561 (2022).
52. Luc, A. & Wencel-Delord, J. One reaction – double stereoinduction: C–H activation as a privileged route towards complex atropisomeric molecules. *Chem. Commun.* **59**, 8159–8167 (2023).

53. Zhang, H.-H., Zhen, T., Liu, S.-J. & Shi, F. Catalytic asymmetric synthesis of atropisomers bearing multiple chiral elements: An emerging field. *Angew. Chem. Int. Ed.* **63**, e202311053 (2024).
54. Portolani, C. et al. Synthesis of atropisomeric hydrazides by one-pot sequential enantioselective and diastereoselective catalysis. *Angew. Chem. Int. Ed.* **61**, e202209895 (2022).
55. Wang, S.-J. et al. Organocatalytic diastereo- and atroposelective construction of N–N axially chiral pyrroles and indoles. *Nat. Commun.* **15**, 518 (2024).
56. Speck, K. & Magauer, T. The chemistry of isoindole natural products. *Beilstein. J. Org. Chem.* **9**, 2048–2078 (2013).
57. Thong, W. L., Shin-Ya, K., Nishiyama, M. & Kuzuyama, T. Discovery of an antibacterial isoindolinone-containing tetracyclic polyketide by cryptic gene activation and characterization of its biosynthetic gene cluster. *ACS Chem. Biol.* **13**, 2615–2622 (2018).
58. Chessari, G. & Hardcastle, I. R. Structure-Based design of potent and orally active isoindolinone inhibitors of MDM2-p53 protein–protein interaction. *J. Med. Chem.* **64**, 4071–4088 (2021).
59. Augner, D., Gerbino, D. C., Slavov, N., Neudçrfl, J.-M. & Schmalz, H.-G. *N*-Capping of primary amines with 2-acylbenzaldehydes to give isoindolinones. *Org. Lett.* **13**, 5374–5377 (2011).
60. Zhang, Y. et al. Chiral phosphoric acid catalyzed asymmetric Ugi reaction by dynamic kinetic resolution of the primary multicomponent adduct. *Angew. Chem. Int. Ed.* **55**, 5282–5285 (2016).
61. Min, C., Lin, Y. & Seidel, D. Catalytic enantioselective synthesis of Mariline A and related isoindolinones through a biomimetic approach. *Angew. Chem. Int. Ed.* **56**, 15353–15357 (2017).
62. You, S.-L., Cai, Q. & Zeng, M. Chiral Brønsted acid catalyzed Friedel–Crafts alkylation reactions. *Chem. Soc. Rev.* **38**, 2190–2201 (2009).
63. Parmar, D., Sugiono, E., Raja, S. & Rueping, M. Complete field guide to asymmetric BINOL-phosphate derived Brønsted acid and metal catalysis: History and classification by mode of activation; Brønsted acidity, hydrogen bonding, ion pairing, and metal phosphates. *Chem. Rev.* **114**, 9047–9153 (2014).
64. Parmar, D., Sugiono, E., Raja, S. & Rueping, M. Addition and correction to complete field guide to asymmetric BINOL-phosphate derived Brønsted acid and metal catalysis: History and classification by mode of activation; Brønsted acidity, hydrogen bonding, ion pairing, and metal phosphates. *Chem. Rev.* **117**, 10608–10620 (2017).
65. Da, B.-C., Xiang, S.-H., Li, S. & Tan, B. Chiral phosphoric acid catalyzed asymmetric synthesis of axially chiral compounds. *Chin. J. Chem.* **39**, 1787–1796 (2021).
66. Fazullina, A. A., Ryapisova, L. V., Kashevarova, L. B. & Fridland, S. V. Reactions of benzaldehyde dimethylhydrazone with phosphorous acids. *Russ. J. Gen. Chem.* **83**, 2119–2121 (2013).
67. Tian, H. et al. Pyrrole-assisted and easy oxidation of cyclic α-amino acid-derived diketopiperazines under mild conditions. *Adv. Synth. Catal.* **353**, 1525–1533 (2011).
68. Petsi, M. & Zografos, A. L. 2,5-Diketopiperazine catalysts as activators of dioxygen in oxidative processes. *ACS Catal.* **10**, 7093–7099 (2020).
69. Breytenbach, J. C. et al. Synthesis and antimicrobial activity of some isoindolin-1-ones derivatives. *Bioorg. Med. Chem. Lett.* **10**, 1629–1631 (2000).
70. Maugeri, C. et al. New anti-viral drugs for the treatment of the common cold. *Bioorg. Med. Chem.* **16**, 3091–3107 (2008).
71. Zhao, X.-Z., Maddali, K., Marchand, C., Pommier, Y. & Burke, T. R. Diketoacid-genre HIV-1 integrase inhibitors containing enantiomeric arylamide functionality. *Bioorg. Med. Chem.* **17**, 5318–5324 (2009).
72. Pereira, N. A. L. et al. Enantiopure indolizinoindolones with in vitro activity against blood- and liver-stage malaria parasites. *ChemMedChem* **10**, 2080–2089 (2015).
73. Bhatia, R. K. Isoindole derivatives: Propitious anticancer structural motifs. *Curr. Top. Med. Chem.* **17**, 189–207 (2016).

Acknowledgements

This work was supported by the National Natural Science Foundation of China (22201073 to X.L., 21925201 to P.-N.L., 22161160319 to P.-N.L., T2322018 to H.X., 22171130 to P.Y., 32171391 to H.X.) and the Fundamental Research Funds for the Central Universities. We thank the Research Center of Analysis and Test of East China University of Science and Technology for help in the characterization. P.Y. acknowledges Shenzhen Science and Technology Program (KQTD20210811090112004) for financial support. Computational work was supported by the Center for Computational Science and Engineering and the CHEM High-Performance Supercomputer Cluster (CHEM-HPC) of the Department of Chemistry, Southern University of Science and Technology.

Author contributions

X.L. conceived, directed the project and wrote the paper. X.-Z.W. and Q.-Y.C. performed and analyzed the experiments. P.Y. and B.S. performed the DFT studies. H.X. designed and performed the biological experiments. P.-N.L. directed the project. All the authors discussed the results and commented on the manuscript.

Competing interests

The authors declare no competing interests.

Additional information

Supplementary information The online version contains supplementary material available at https://doi.org/10.1038/s41467-025-56838-2.

Correspondence and requests for materials should be addressed to Xingguang Li, Peiyuan Yu or Pei-Nian Liu.

Peer review information *Nature Communications* thanks the anonymous reviewers for their contribution to the peer review of this work. A peer review file is available.